

**Document Version**

Final published version

**Licence**

Dutch Copyright Act (Article 25fa)

**Citation (APA)**

Yong, A. X. H., Endruweit, A., George, A., May, D., Aksoy, Y. A., Caglar, B., Dransfeld, C., Masania, K., Yuksel, O., & More Authors (2026). Through-thickness compaction response of reinforcement fabrics: Development of a test standard. *Composites Part A: Applied Science and Manufacturing*, 200, Article 109348. <https://doi.org/10.1016/j.compositesa.2025.109348>

**Important note**

To cite this publication, please use the final published version (if applicable).  
Please check the document version above.

**Copyright**

In case the licence states “Dutch Copyright Act (Article 25fa)”, this publication was made available Green Open Access via the TU Delft Institutional Repository pursuant to Dutch Copyright Act (Article 25fa, the Taverne amendment). This provision does not affect copyright ownership.  
Unless copyright is transferred by contract or statute, it remains with the copyright holder.

**Sharing and reuse**

Other than for strictly personal use, it is not permitted to download, forward or distribute the text or part of it, without the consent of the author(s) and/or copyright holder(s), unless the work is under an open content license such as Creative Commons.

**Takedown policy**

Please contact us and provide details if you believe this document breaches copyrights.  
We will remove access to the work immediately and investigate your claim.

**Green Open Access added to [TU Delft Institutional Repository](#)  
as part of the Taverne amendment.**

More information about this copyright law amendment  
can be found at <https://www.openaccess.nl>.

Otherwise as indicated in the copyright section:  
the publisher is the copyright holder of this work and the  
author uses the Dutch legislation to make this work public.



## Through-thickness compaction response of reinforcement fabrics: Development of a test standard

A.X.H. Yong<sup>a,\*</sup>, A. Endruweit<sup>b</sup>, A. George<sup>c</sup>, D. May<sup>d</sup>, Y.A. Aksoy<sup>e</sup>, M.A. Ali<sup>f</sup>,  
T. Allen<sup>g</sup>, M. Bender<sup>h</sup>, M. Bodaghi<sup>i,j</sup>, B. Caglar<sup>e</sup>, H. Caglar<sup>k</sup>, A. Chiminelli<sup>l</sup>,  
S. Comas-Cardona<sup>m</sup>, R. de Ribains<sup>n</sup>, J. Dittmann<sup>o</sup>, C. Dransfeld<sup>e</sup>, E. Fauster<sup>h</sup>,  
A. Guilloux<sup>p</sup>, P. Hubert<sup>q</sup>, S. Idapalapati<sup>k</sup>, J. Ivens<sup>r</sup>, J. Janzen<sup>s</sup>, Y. Jiang<sup>t</sup>, T. Khan<sup>f</sup>,  
M. Laspalas<sup>l</sup>, F. LeBel<sup>t</sup>, J. Lee<sup>g</sup>, X. Liu<sup>r</sup>, M. Lizaranzu<sup>l</sup>, S.V. Lomov<sup>r</sup>, C. López<sup>l</sup>,  
K. Masania<sup>e</sup>, V. Michaud<sup>n</sup>, P. Middendorf<sup>o</sup>, S. Miguel<sup>l</sup>, S.S. Narayana<sup>q</sup>, C.H. Park<sup>i</sup>,  
S. Ravisankar Padma<sup>k</sup>, L. Riffard<sup>t</sup>, C. Pinger<sup>t</sup>, V. Rougier<sup>n</sup>, H. Sas<sup>v</sup>, D. Sayinbas<sup>w</sup>,  
P. Sousa<sup>r</sup>, M. Sozer<sup>w</sup>, M. Steinhardt<sup>u</sup>, R. Umer<sup>f</sup>, J.D. Vincent<sup>a</sup>, V. Werlen<sup>x</sup>, O. Yuksel<sup>e</sup>

<sup>a</sup> National Physical Laboratory, United Kingdom

<sup>b</sup> University of Nottingham, UK

<sup>c</sup> Brigham Young University, USA

<sup>d</sup> Faserinstitut Bremen e.V., University of Bremen, formerly Leibniz-Institut für Verbundwerkstoffe GmbH, Germany

<sup>e</sup> TU Delft, Netherlands

<sup>f</sup> Khalifa University of Science and Technology, United Arab Emirates

<sup>g</sup> University of Auckland, New Zealand

<sup>h</sup> Technical University of Leoben, Austria

<sup>i</sup> IMT Nord Europe, France

<sup>j</sup> Luxembourg Institute of Science and Technology (LIST), Luxembourg, Germany

<sup>k</sup> Nanyang Technological University, Singapore

<sup>l</sup> ITAINNOVA, Spain

<sup>m</sup> Centrale Nantes, France

<sup>n</sup> Ecole Polytechnique Federale de Lausanne, Switzerland

<sup>o</sup> University of Stuttgart, Germany

<sup>p</sup> TENSYL, France

<sup>q</sup> McGill University, Canada

<sup>r</sup> KU Leuven, Belgium

<sup>s</sup> Leibniz-Institut für Verbundwerkstoffe GmbH, Germany

<sup>t</sup> Centre Technologique en Aérospatiale (CTA), Canada

<sup>u</sup> TU Munich, Germany

<sup>v</sup> Sabanci University, Turkey

<sup>w</sup> Koc University, Turkey

<sup>x</sup> FHNW University of Applied Sciences and Arts Northwestern Switzerland, Switzerland

### ARTICLE INFO

#### Keywords:

Fabric/textiles  
Mechanical testing  
Compressibility

### ABSTRACT

Characterisation of the compaction response of reinforcement fabrics is an important component in the design of composite manufacturing processes. To standardise a best practice method, 22 international organisations participated in an exercise to assess the viability and reproducibility of the method discussed in this work. All participants were supplied with the same multiaxial E-glass fibre non-crimp fabric and instructed to measure the compaction stress as a function of the specimen thickness following a set of guidelines. The scatter in results between participants was quantified in terms of the coefficient of variation (CV). The CV of the maximum compaction stress determined at a target specimen thickness of 3 mm (for 10 fabric layers) was 42 % for dry specimens and 46 % for wet specimens, however this was influenced by scatter in the thickness values, which

\* Corresponding author.

E-mail address: [ana.yong@npl.co.uk](mailto:ana.yong@npl.co.uk) (A.X.H. Yong).

<https://doi.org/10.1016/j.compositesa.2025.109348>

Received 7 July 2025; Received in revised form 3 October 2025; Accepted 5 October 2025

Available online 8 October 2025

1359-835X/© 2025 Elsevier Ltd. All rights reserved, including those for text and data mining, AI training, and similar technologies.

deviated from the target. The CV of the specimen thickness at a compaction stress of  $10^5$  Pa was 4 %. In addition, a power law model and a model based on bending of beams were fitted to the compaction curves. Both generally produced fits with high values of the coefficient of determination. The observed level of scatter is thought to be caused by issues with the implementation of the procedures and by variability in the specimen properties, as well as the very steep variation of the force/thickness curve at the required target. The guidelines used here aim to minimise inaccuracies in the test method and will be proposed as a test protocol for standardisation.

## 1. Introduction

The behaviour during through-thickness compression of the textile reinforcements used in the manufacture of fibre-reinforced composites is an important property to be understood. For composites manufacturing processes using a fixed compaction pressure and a flexible mould, such as Vacuum Infusion, measuring the relationship between reinforcement thickness and compaction pressure provides details on the attainable composite thickness and fibre volume fraction. Further, information on the impact of compression on the resin flow during manufacture can be provided, which can be useful in the design of the process. Alternatively, for closed mould methods such as Resin Transfer Moulding, these measurements provide an insight into the closing force on the tool at a set thickness, where the thickness informs the fibre volume fraction of the finished part. Here, informed design of the manufacturing process and tool can lead to significant time and cost savings over a trial-and-error approach.

Fabric behaviour during compression has been well-characterised, with a number of models available to describe the response [1–15]. It is well known that the compaction load will undergo a relaxation over time when a fabric is compressed to a constant thickness, indicating a quasi-viscoelastic behaviour. Another implication of this behaviour is the stress hysteresis effect, where the compaction pressure at a given specimen thickness is higher during the loading than during unloading, and repeated loading and unloading reduces the peak pressure on the tool [3]. As a result, cyclic compaction can be used to reduce the compaction pressure required for a desired part thickness or fibre volume fraction.

In addition, the compaction response is different for dry and wet fabrics, which is of particular importance to manufacturing methods such as Vacuum Infusion, where the wet part of the reinforcement will typically compress to a smaller thickness under atmospheric pressure than the dry part. Hence, information for both the dry and wetted reinforcement is relevant [1,3,16].

In multi-layer fabric stacks, the effect of nesting occurs at the interfaces between adjacent layers, which corresponds to in-plane displacements of the layers relative to each other. This results in a reduction in effective average layer thickness (compared to a single fabric layer) and a decrease in compaction force required to obtain a given stack thickness [17]. As this effect is stochastic in nature (and hard to control), it may result in a significant scatter in properties for small numbers of layers and a convergence for large numbers of layers.

While the behaviour of textile reinforcements in compression is well-understood, there exists no standardised test method for its characterisation. In order to address this issue, the first interlaboratory trial on the reinforcement compaction response was completed in 2021 with the aims of understanding and identifying the potential sources of variability between users [18]. In this first benchmark exercise, the coefficient of variation in the maximum compaction stress at a given target thickness of 3 mm for a stack of 10 to 14 layers of two different fabrics ranged from 38 % to 58 %. A number of parameters were identified, and the main source of variation was found to be inaccuracy in the control and/or measurement of the specimen thickness, i.e. the distance between compression platens, and their parallelism, as well as the method to saturate the preform in the wet conditions. Therefore, it was concluded that a second benchmark exercise be carried out with stricter guidelines on how the specimen thickness be controlled and measured.

In this work, the known principles of the compression test, i.e. compression of a fabric at a set speed to a defined thickness, again provide the methodology for establishing a best practice method for standardisation. This builds on the work of the first benchmark exercise with refined elements of the test setup to ensure the best testing protocol for users. The list of participants to the second benchmark is provided in Table 1; 14 of the current participants were also part of the first benchmark exercise [18].

## 2. Materials

The textile material characterised in this study was a multiaxial E-glass fibre non-crimp fabric (NCF) with pillar stitch supplied by Saertex (superficial density  $444 \text{ g/m}^2$ ). Each participant was sent a length of the same fabric, which was selected to match the non-crimp fabric used in the first benchmark exercise. Whilst this fabric was nominally the same, further assessment of the materials showed slight differences in the yarn count per unit of distance due to the change in batch. Further details of the fabrics used in the original and current benchmarks are given by May et al. [19] and Yong et al. [20], respectively.

Participants were instructed to use the Dow Corning Xiameter PMX-200 100 cst silicone oil in the wet compression tests, which they were required to source from their local supplier. The selected oil was kept consistent with the previous series of benchmark exercises on reinforcement compaction and permeability measurement [18–21]. Silicone oil is used in these types of tests as its viscosity is comparable to that of liquid resin systems used in Liquid Composite Moulding and does not change with time (as long as the temperature is constant). Participants were free to characterise the viscosity of the silicone oil or send a sample to the National Physical Laboratory (UK) for characterisation.

**Table 1**  
List of participants.

Participant ID	Institution	Country
1	Montanuniversitat Leoben	Austria
2	KU Leuven	Belgium
3	Centre Technologique en Aérospatiale (CTA)	Canada
4	McGill University	Canada
5	Centrale Nantes	France
6	IMT Nord Europe	France
7	TENSYL	France
8	Leibniz-Institut für Verbundwerkstoffe	Germany
9	TU Munich	Germany
10	University of Stuttgart	Germany
11	TU Delft	Netherlands
12	University of Auckland	New Zealand
13	Nanyang Technological University	Singapore
14	Aragon Institute of Technology (ITA)	Spain
15	Ecole Polytechnique Federale de Lausanne	Switzerland
16	FHNW University of Applied Sciences and Arts Northwestern Switzerland	Switzerland
17	Koc University	Turkey
18	Sabanci University	Turkey
19	Khalifa University of Science and Technology	UAE
20	National Physical Laboratory	UK
21	University of Nottingham	UK
22	Brigham Young University	USA

### 3. Methods

#### 3.1. Specimen preparation

The samples for the compression tests consist of a stack of cut-outs from the fabric. Samples were to be prepared using 10 layers of fabric, all having the same orientation. It is known that nesting can play a significant role in the fabric behaviour, therefore the number of layers must be kept the same for comparable data [17]. This was shown by Pearce and Summerscales, who conducted compaction tests at different numbers of reinforcement layers in the specimens and fitted power-law curves to the measured data for the compaction pressure as a function of the fibre volume fraction. They found that the number of layers used during testing changes the exponent of power-law fits applied to compression data [22]. Specifically, the value of the exponent tended to increase with increasing number of layers, indicating a more compliant stack when thicker, getting to an asymptotic behaviour when the number of layers exceeds a sufficient value Fig. 1.

Participants were free to choose the areal dimensions of the specimens provided they were of edge length or diameter in the order of 100 mm to ensure that the sample area was larger than the repeated unit cell (RUC) of the fabric, and smaller than the compression platens to be used, i.e. the complete stack area is compressed in testing. This is a widely used approach, but many studies have also been reported in literature where the samples are larger than the platens. If the platens are smaller than the sample, it could be argued that the compression area is perfectly defined by the platen area. However, there is no sharp edge between the compressed area and the surrounding uncompressed area. Within a transition area the part of the sample not directly in contact with the platens will nevertheless be deformed. This deformation requires an undefined amount of force so that the correlation between the applied load and the measured thickness is affected. If the platens are larger than the sample, such effects are not an issue, and the target sample area is used for calculation of the pressure (note that the expression “compaction stress” will be used in the following to be consistent with previous work [18]). It should be noted that in the condition where the sample is smaller than the platen, there may be some edge effects caused by factors such as the local reduction in compaction stiffness of the sample stack at its edge due to cuts to the stitching and fibre tows, or misalignment of the layers in the sample stack at the edges. This means that utmost care must be taken to ensure congruent stacking and to avoid handling-induced distortion and/or fringe out, i.e. loss of fiber bundles along the edges. Therefore, it was mandatory to prepare specimens using a precise cutting method such as a die cutter or CNC cutter. A further benefit of the platens being larger than the specimens is that a specimen size and shape can be prescribed without the necessity of having to manufacture platens for this specific specimen. This advantage in terms of practicality can be relevant for further standardization efforts. With regards to fluid-saturated (wet) compaction tests, the free flow of the test fluid from the specimen into the space between the platens can be another relevant advantage. If the fluid needs to flow through surrounding textile, the effect of the additional force required to squeeze fluid through the specimen (which depends on the reinforcement in-plane permeability) could cause errors in compaction stress measurement.

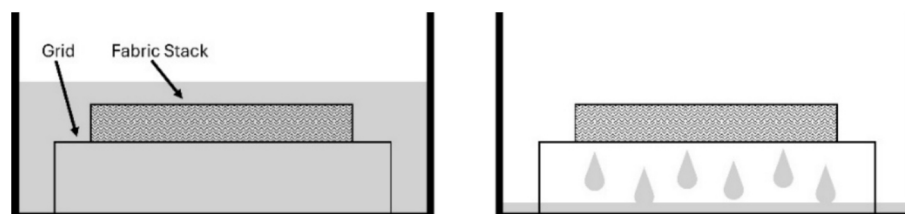


Fig. 1. Schematic diagrams detailing wet sample preparation. Left: wetting in oil bath. Right: draining.

#### 3.2. Sample wetting

Tests were carried out on both dry and wet specimens. To prepare the wet specimens, participants were instructed to immerse each specimen stack in the specified silicone oil for 15 min, to allow enough time for each layer to become fully saturated. Specimens were then removed from the oil bath and drained for a further 15 min to remove excess fluid. The immersion and draining times were mandatory, to ensure consistency of specimen saturation levels between participants. This is a further iteration of the method used in the first benchmark exercise, where the draining times were not prescribed. A higher degree of variation was seen in the wet tests compared to dry tests in that first benchmark (38 % for dry tests on the two fabrics used compared to 40 % and 50 % in the wet tests), which were explained with the resultant variation in degree of saturation [18].

#### 3.3. Equipment

It was mandatory for testing to be carried out using a Universal Test Machine (UTM). The compression platens were required to be larger than the fabric specimens (see above). A minimum width or diameter of 50 mm was required for the platens. An example of a typical compression test setup is shown in Fig. 2.

Compliance in the test set-up may have an effect on the measured platen displacement, if the measurement is based on the cross-head displacement. Hence, thickness measurements were to be carried out using a direct method, such as with a Linear Variable Displacement Transformer (LVDT) for measuring the distance between the compression platens or with an extensometer. If a direct method is not employed, a correction needs to be applied to the recorded cross-head displacement data. In the first international benchmarking exercise, inaccuracies in the thickness measurement and high variability in the approach towards machine compliance correction were found to be a source of scatter in the results, while lower variability was observed between the group of participants using direct thickness measurement methods [18]. The use of a direct method was intended to reduce the effect of machine compliance on the measurement results.

#### 3.4. Parallelism

Use of a lockable self-aligning platen was mandatory for this study to ensure parallelism between compression platens, where any offset from parallel would cause a variation in thickness across the compressed specimen and result in erroneous data. Participants were asked to record evidence of the parallelism using pressure film, such as Fujifilm Prescale™. Here, participants were instructed to prepare a sheet of pressure film larger than the platen contact area and apply the same compressive load as used in the preliminary compliance measurements. It should be expected that for parallel platens, the distribution of the compaction stress is uniform, and no significant gradient in colour intensity can be seen imprinted on the pressure film after compression.

#### 3.5. Machine compliance

Although the use of a direct thickness measurement method was



Fig. 2. Example compression test setup including lockable self-aligning platen and LVDTs.

mandatory, participants were required to characterise the machine compliance to provide supplementary information on the stability of the test setup [23]. Participants were required to record 3 loading and unloading cycles (without reinforcement specimen) immediately before and after each test series. To carry out these measurements, the platens were pressed together at a speed of 0.5 mm/min to a load higher than that used in the reinforcement compression tests (pre-test), and to the same load as in testing (post-test) [24].

### 3.6. Test

Participants were instructed to compress the specimen at a speed of 1 mm/min to a target thickness of 3 mm and then separate the platens at the same speed, with no holding phase, as the holding phase was not considered to bring any added value in the first benchmark exercise. Here, the specimen thickness is considered to be identical to the distance between compression platens measured by the direct method of choice for the participant (e.g. LVDT). The compaction force was to be recorded during the test and the compaction stress to be calculated from the force and the specimen area. It was mandatory for all participants to use the same compression speed as the peak stress measured in reinforcement compaction tests typically increases with compression speed [1,3,25].

This test was to be repeated five times each for the two specimen conditions (wet and dry), using a new specimen for each test. The use of a new specimen for each test was imperative due to the known occurrence of a stress hysteresis effect when the same specimen is loaded and

unloaded more than once [3].

## 4. Results

### 4.1. Participant compliance with guidelines

To assess the suitability and reproducibility of the proposed test method for standardisation, participants were instructed to follow the guidelines listed in Section 3. Table 2 provides details of the individual test setup arrangements for each participant and Table 3 shows participant compliance to the guidelines. Additional details, such as specimen dimensions, are provided in Appendix A.

One participant (participant 17) submitted data using an alternative compression method for comparison. In this method, the participant compressed samples using a vacuum bag at different levels of vacuum and monitored the thickness changes using an optical technique, structured light scanning (SLS). Following this procedure, the specimens experienced different (increasing) stress levels and relaxation phases (for a duration of 30 s) at each level. The maximum compaction stress was 75 kPa before the stress was reduced following a reversed sequence of the same levels. Each specimen went through three compression cycles. Hence, the results cannot be expected to be comparable with the results relating to the prescribed load cycle.

### 4.2. Preliminary analysis of compression curves

For illustration of typical experimental results, data recorded by one of the participants for the compaction stress,  $\sigma_c$ , as a function of the specimen thickness,  $t$ , are plotted in Fig. 3 (for dry and wet tests). The curves show generally good repeatability between the five tests in each series. The compaction stress at any given specimen thickness is higher during the loading phase than during the unloading phase, confirming the hysteretic behaviour of the specimens.

For three participants (participants 2 to 4), the recorded  $\sigma_c(t)$  curves show non-zero values of the compaction stress even when the specimens are not compacted (for large values of  $t$ ), i.e. there is an offset in the data that is not attributable to the compaction stress likely caused by failure

Table 2

Test setup for each participant. DIC indicates Digital Image Correlation.

ID	Load cell (kN)	Thickness measurement	Platen shape	Specimen shape	Larger platen
1	30	LVDT	Circle	Circle	Yes
2	30	Laser	Circle	Square	Yes
3	100	LVDT	Square	Square	Yes
4	5	LVDT and DIC	Rectangular	Square	Yes
5	100	LVDT	Circle	Square	Yes
6	100	LVDT	Circle	Circle	Yes
7	20	LVDT	Circle	Circle	Yes
8	250	Camera system – DIC	Circle	Circle	Yes
9	250	Video extensometer	Square	Square	Yes
10	20	LVDT	Square	Square	Yes
11	250	LVDT	Circle	Circle	Yes
12	200	LVDT	Circle	Square	Yes
13	50	UTM	Circle	Square	Yes
14	100	Video extensometer	Circle	Circle	Yes
15	10	LVDT	Circle	Square	Yes
16	100	Camera	Circle	Circle	Yes
17	N/A	Structured light scanning	N/A	Circle	N/A
18	Not disclosed	Not disclosed	Circle	Circle	Yes
19	5	LVDT	Circle	Circle	Yes
20	250	LVDT	Circle	Circle	Yes
21	50	LVDT	Circle	Circle	Yes
22	5	Laser	Square	Circle	Yes

**Table 3**  
Participant compliance with guidelines.

ID	n layers = 10	Edge length	Fabric cutting	Use of UTM	Self-aligning platen	Pressure film	Direct thickness sensor	Larger platen	Overall score
1	Yes	Yes	Yes	Yes	Yes	Yes	Yes	Yes	Yes
2	Yes	Yes	No	Yes	Yes	No	Yes	Yes	No
3	Yes	Yes	Yes	Yes	No	Yes	Yes	Yes	No
4	Yes	Yes	No	Yes	No	Yes	Yes	Yes	No
5	Yes	Yes	No	Yes	Yes	No	Yes	Yes	No
6	Yes	Yes	Yes	Yes	Yes	Yes	Yes	Yes	Yes
7	Yes	Yes	Yes	Yes	Yes	No	Yes	Yes	No
8	Yes	Yes	Yes	Yes	Yes	Yes	Yes	Yes	Yes
9	Yes	Yes	Yes	Yes	Yes	Yes	Yes	Yes	Yes
10	Yes	Yes	Yes	Yes	Yes	Yes	Yes	Yes	Yes
11	Yes	Yes	Yes	Yes	Yes	Yes	Yes	Yes	Yes
12	Yes	Yes	Yes	Yes	Yes	Yes	Yes	Yes	Yes
13	Yes	Yes	Yes	Yes	Yes	No	Yes	Yes	No
14	Yes	Yes	Yes	Yes	Yes	Yes	Yes	Yes	Yes
15	Yes	Yes	Yes	Yes	Yes	Yes	Yes	Yes	Yes
16	Yes	Yes	Yes	Yes	Yes	Yes	Yes	Yes	Yes
17	Yes	Yes	Yes	No	No	No	Yes	Yes	No
18	Yes	Yes	--	Yes	--	Yes	--	Yes	--
19	Yes	Yes	Yes	Yes	No	Yes	Yes	Yes	No
20	Yes	Yes	Yes	Yes	Yes	Yes	Yes	Yes	Yes
21	Yes	Yes	Yes	Yes	Yes	Yes	Yes	Yes	Yes
22	Yes	Yes	Yes	Yes	Yes	Yes	Yes	Yes	Yes

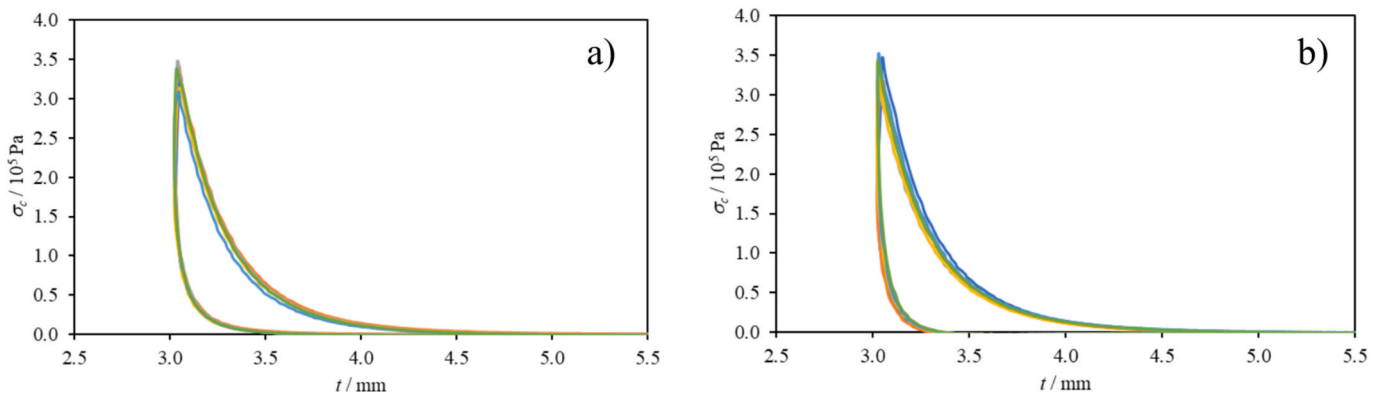


**Fig. 3.** Examples of recorded data (five specimens) for the compaction stress,  $\sigma_c$ , as a function of the specimen thickness,  $t$ ; a) dry tests; b) wet tests. Each coloured line represents one test of a different specimen in a series.

to zero the instrument prior to test. For participant 2, this offset in  $\sigma_c$  is negative in loading and unloading, but for participants 3 and 4, it is positive in loading and negative in unloading. For participant 2, the offset is consistently  $-1.3 \times 10^4$  Pa in all tests. For participant 3, it is approximately  $2.3 \times 10^4$  Pa and  $-2.2 \times 10^4$  Pa in loading and unloading in the dry tests. In the wet tests, it is approximately  $1.2 \times 10^4$  Pa and  $-1.1 \times 10^4$  Pa, respectively. For participant 4, the offset is on average approximately  $1.7 \times 10^4$  Pa in dry loading and  $1.7 \times 10^3$  Pa in dry unloading. The negative values in the curves from the wet tests were not included in the data.

#### 4.3. Reproducibility of data

For each participant, the average of the maximum compaction stress,  $\sigma_{c,max}$ , and the average thickness at maximum compaction stress,  $t_{max}$ , are presented in Fig. 4(a) for the dry tests and Fig. 4(b) for the wet tests. Note that data for participant 17, who implemented a different loading cycle, is included in the figure for comparison. Considering all data with the exception of participant 17,  $t_{max}$  and  $\sigma_{c,max}$  are on average higher for the dry tests than for the wet tests (by 0.1 % and 1.0 %, respectively). This means that the dry specimens are less likely to be compressed to the target thickness and that a higher compressive stress is required to obtain this thickness. This is consistent with wet specimens being easier to compress than dry specimens, although the effect is small.

Evaluating data obtained by all participants with the exception of participant 17, the average value of the maximum compaction stress for the dry and wet tests was  $3.45 \times 10^5$  Pa and  $3.41 \times 10^5$  Pa, respectively. The coefficient of variation on the as-received data was 46 % and 42 %, respectively. It should be noted that some of the returned datasets contained errors in data reduction, such as the incorrect use of units for the compaction stress, which have been corrected here. The results presented in Fig. 4 show that, despite the test guidelines to compress to a set thickness of 3 mm, there was scatter in the thickness values at maximum compaction stress (3.0 % for the dry test and 2.8 % for the wet tests at average values of 3.01 mm and 3.00 mm, respectively). Note that the data set is quite similar to that found in the first benchmark, where an average compaction stress for a target thickness of 3 mm was  $3.7 \times 10^5$  Pa and  $3.17 \times 10^5$  Pa for dry and wet cases respectively, and with CV of 38 % and 40 %.

For comparison, participant 17 found average values for  $t_{max}$  of 3.10 mm and 3.12 mm for dry and wet tests (only considering the first compaction cycle), respectively. The corresponding coefficients of variation were 0.7 % and 0.8 %. In general,  $t_{max}$  seems to occur at lower compaction stress than for participants following the prescribed load cycle (although there may be a few outliers). This confirms the effect of the load cycle on the compaction response.

In order to compare the results using a single variable, the values for the measured thickness at a compaction stress of  $10^5$  Pa (during the

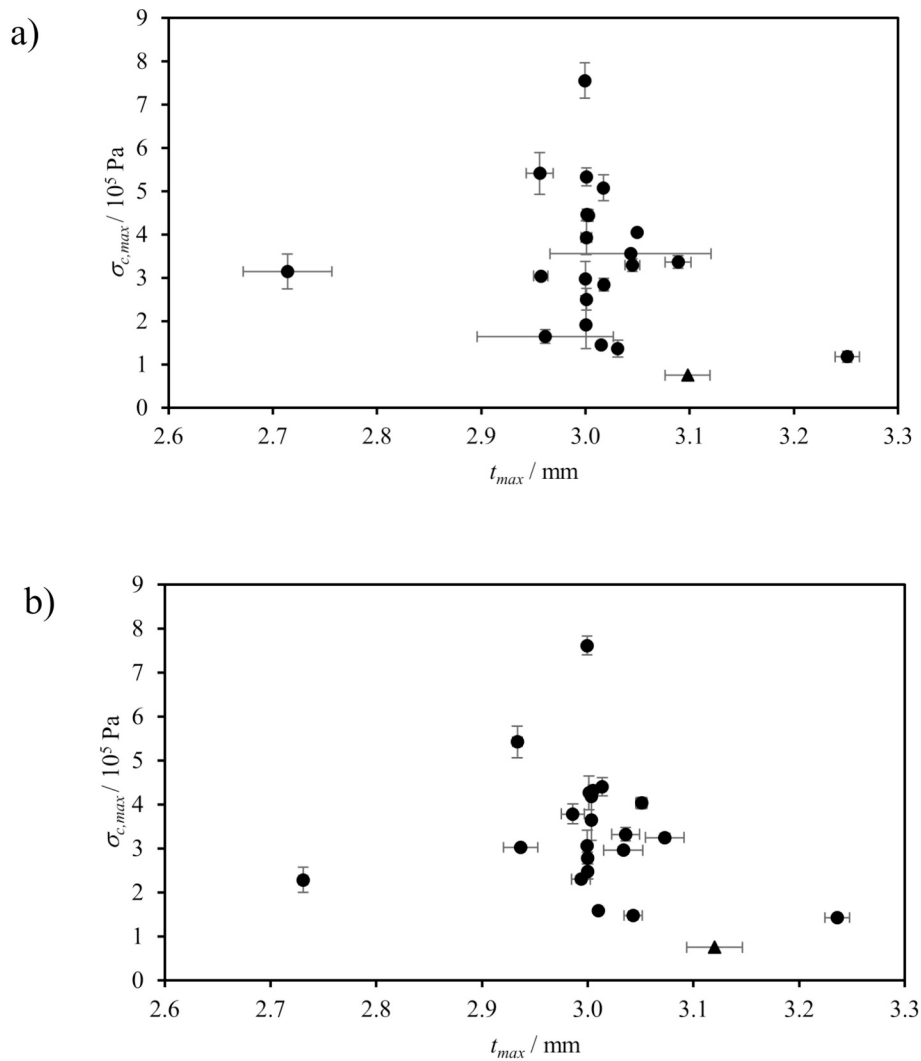


Fig. 4. Maximum compaction stress,  $\sigma_{c,max}$ , at the corresponding specimen thickness,  $t_{max}$ , for all participants; a) dry tests and b) wet tests. Error bars indicate the standard deviation of the series of five repeats for each participant. Triangular symbol indicates data by participant 17.

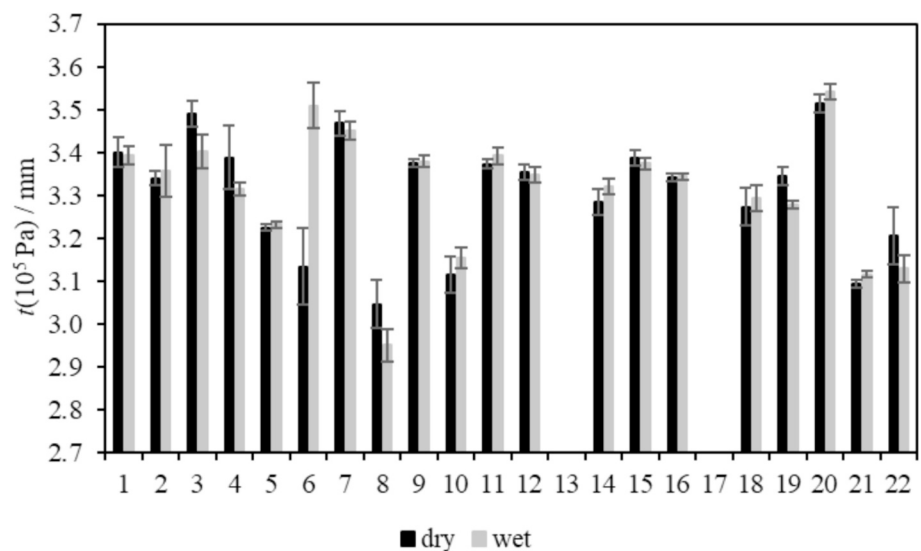


Fig. 5. Specimen thickness,  $t$ , at a compaction stress of  $10^5 \text{ Pa}$ . Error bars indicate standard deviation.

loading phase) are presented in Fig. 5. Participant 13 did not provide the recorded curves, and participant 17 did not achieve  $10^5$  Pa during testing. Therefore, both participants show no reading in the figure. For the remaining datasets, the coefficient of variation in thickness at a compaction stress of  $10^5$  Pa is 4 % for both the dry and wet tests. On average,  $t(10^5 \text{ Pa})$  is 0.1 % lower for dry specimens than for wet specimens, which seems not to be consistent with the observations for  $t_{max}$  and  $\sigma_{c,max}$ . Here, it is to be considered that the slope of the  $\sigma_c(t)$  curves (as in Fig. 3) varies across the range of  $t$ . If  $t_{max}$  is higher for dry than for wet specimens for a participant, this does not necessarily mean that  $t(10^5 \text{ Pa})$  is also higher for dry than for wet specimens. This apparent inconsistency is a general shortcoming of the comparison based on single points on the compaction curves.

The generally small difference between dry and wet specimens is consistent with previous observations [18] which indicated that the effect of wetting (i.e. lubrication) on the fabric compaction response is less significant for NCFs than for woven fabrics, as the fibre fixation is generally stronger in the NCF and there is a lower degree of fibre reordering.

#### 4.4. Comparison of machine compliance curves

Machine compliance describes the deformation of the entire test machine setup, e.g. movement of the grips and couplings. Compliance curves, recorded during loading of the setup without a specimen, show the movement at each given load that can be attributed to this deformation. The machine compliance curves recorded before and after each test series were inconsistent between participants (as also observed in the previous compression benchmark study [18]). It is thought that different designs of the self-aligning platens result in different shapes of the compliance curves. Eventually, the compliance curves were ignored here.

## 5. Discussion

### 5.1. Model fitting

For comparison of results obtained by different participants, the maximum compaction stress and the corresponding specimen thickness can be used (as in Fig. 4), or another descriptor can be defined, e.g. the specimen thickness at a given compaction stress (as in Fig. 5). However, these approaches describe the fabric compaction response based on one single value and do not give a full picture of the behaviour. It is to be considered that the slope of the curves of acquired raw data (as in Fig. 3) is steep at high compaction levels. Hence, the scatter in data points for the maximum stress and the corresponding specimen thickness may be significant, while the full  $\sigma_c(t)$  curves show high levels of similarity. Comparing the parameters describing the curve shapes may be more indicative of the compaction response than a single point on the curves. Different models exist to create curves describing the compaction behaviour, where a power-law model and a model proposed by Gutowski et al. [26] are used frequently [27–30]. As a large number of compaction stress-thickness curves were acquired in this study, the data were used to check the accuracy of fitting these two frequently used compaction models.

A simple power law was fitted to the thickness,  $t$ , and compaction stress,  $\sigma_c$ , data acquired by the participants, as carried out in the previous benchmark:

$$t = A \left( \frac{\sigma_c}{10^5 \text{ Pa}} \right)^B \quad (1)$$

This was done for both loading (increasing compressive force) and unloading (decreasing compressive force). In this model, the scalar  $A$  represents the specimen thickness at a normalised compaction stress of unity (here, measured stress,  $\sigma_c$ , divided by  $10^5$  Pa). The exponent  $B$

indicates how much the thickness changes with compaction stress. To preclude data points where the sample is under insignificant compression, only data measured at stresses above 1 kPa was used for the data fits. The fitted constants for both  $A$  and  $B$  are shown in Fig. 6, for both loading and unloading, for both dry and wet testing. The data for participant 13 is missing from this graph as force–displacement curves recorded by the UTM was not provided, and a curve fit could not be produced. The data for participant 17 is included here but is kept separately at the side of the chart due to the significant deviation in the test method for this participant. The fit constants for the curves recorded in loading show outliers in participants 3 and 4, especially in the values of  $B$ , where there is generally more scatter than in the values of  $A$ .

Values of the coefficient of determination,  $R^2$ , indicating the quality of the power law fits, are shown in Fig. 7. The unloading data for participants 5 and 22 is omitted due to incomplete data during the unloading phase and thus low fit quality. The  $R^2$  values indicate good fit quality, apart from the outliers (participants 3 and 4), with usually better fits during dry testing compared to wet (for 22 of 42 data sets), and usually better fits in loading compared to unloading (for 34 of 42 data sets). The occurrence of outliers is a result of the positive offsets in the  $\sigma_c(t)$  curves in loading, which does not allow high-quality power law fits to be found. Negative offsets do not affect the fit quality for the unloading curves (also for participant 2).

The average values and standard deviations of the averages of  $A$  and  $B$  across the 5 tests for each participant are given in Tables 4 and 5. In addition, the corresponding coefficients of variation (CV) are given. The data is presented both with (Table 4), and without (Table 5) the two outliers, participants 3 and 4. This table further emphasizes the greater scatter in the exponent  $B$  compared to the factor  $A$ . This implies that the scatter in predicted thickness will increase with increasing compaction stress, as is evident from the model predictions at 200 kPa and 300 kPa included in the Table (where the CV of the predicted thickness tends to be higher for 300 kPa than for 200 kPa). The fit constants from dry and wet testing were nearly identical for most laboratories. With the two outliers excluded, the average ratio  $A_{dry}/A_{wet}$  was 1.00 for loading and 0.99 for unloading. The ratio  $B_{dry}/B_{wet}$  was 0.90 for loading and 1.81 for unloading.

The power law fit is a phenomenological model, i.e. the influence of all mechanical effects on the fabric compaction behaviour is lumped together in the fitting constants.

To explore the relationship between compaction stress and fibre volume fraction,  $V_f$ , which is of particular practical relevance in composites processing, the commonly used fit,

$$\sigma_c = KV_f^n \quad (2)$$

was applied to the stress as measured. Using the same experimental data for  $t$  as above, the fibre volume fraction was calculated according to

$$V_f = \frac{m_f}{tA_f\rho_f} \quad (3)$$

where  $m_f$  is the mass of the specimen,  $A_f$  the specimen area, and  $\rho_f$  the fibre density, which is taken as  $2550 \text{ kg/m}^3$ . When fitting Eq. (2) to data for  $\sigma_c(V_f)$ , fibre volume fractions between 0.3 and 0.5 were considered in cases where log–log plots of the data were not sufficiently linear.

The average value of  $n$  (for all participants except 13) was found to be  $11.8 \pm 2.1$  for dry compression, and  $11.0 \pm 1.1$  for wet compression. As expected from comparison of Eqs. (1) and (2), values of  $n$  are approximately consistent with  $-1/B$ . The average value of the factor  $K$ , which corresponds to the stress at a hypothetical fibre volume fraction of 1, was found to be  $(7.6 \pm 1.5) \times 10^5$  Pa, and  $(7.1 \pm 1.0) \times 10^5$  Pa, respectively. The values of  $n$  are within the range reported in the literature for compression of fabrics with oriented continuous fibres. Results are presented in Fig. 8.

The model proposed by Gutowski et al. [26] was also fitted to the data, which is derived based on the assumption that the fibre bundles in

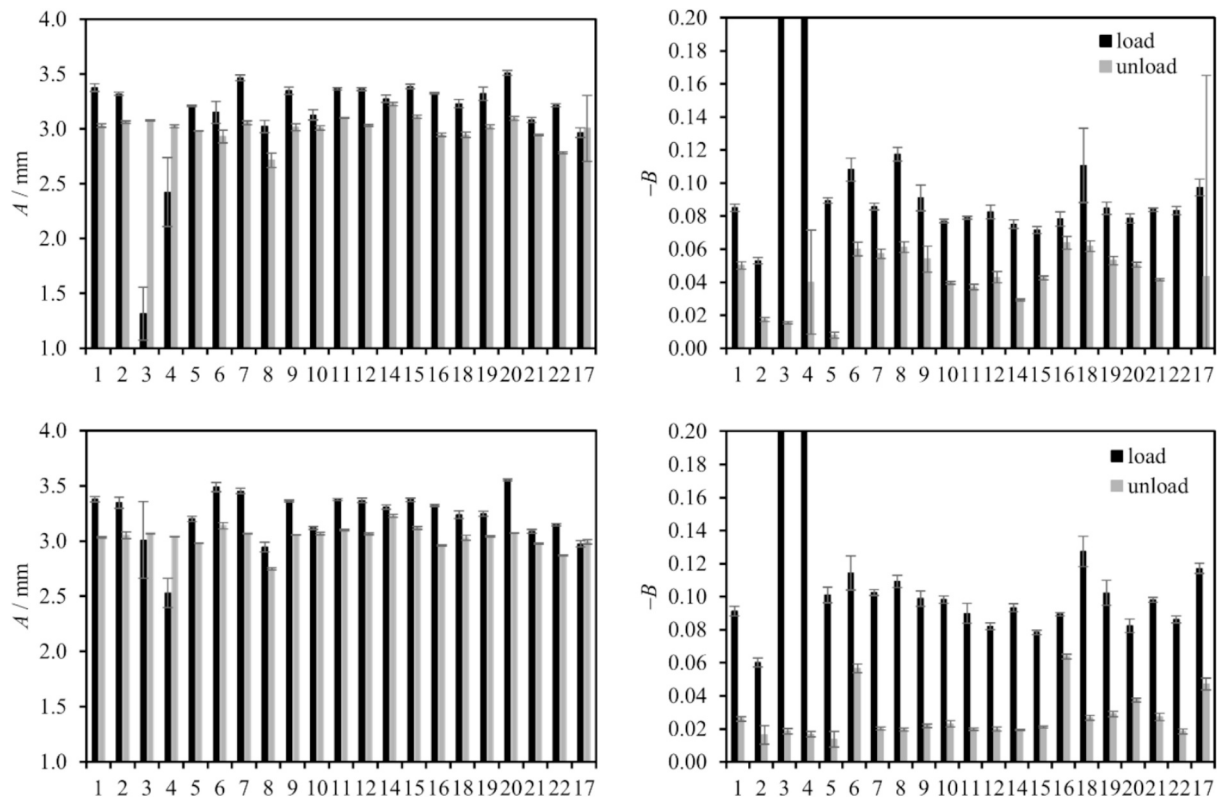


Fig. 6. Power law fit constants,  $A$  and  $B$ , for dry (top) and wet (bottom) test data. Error bars represent the standard deviation across the 5 tests for each participant.

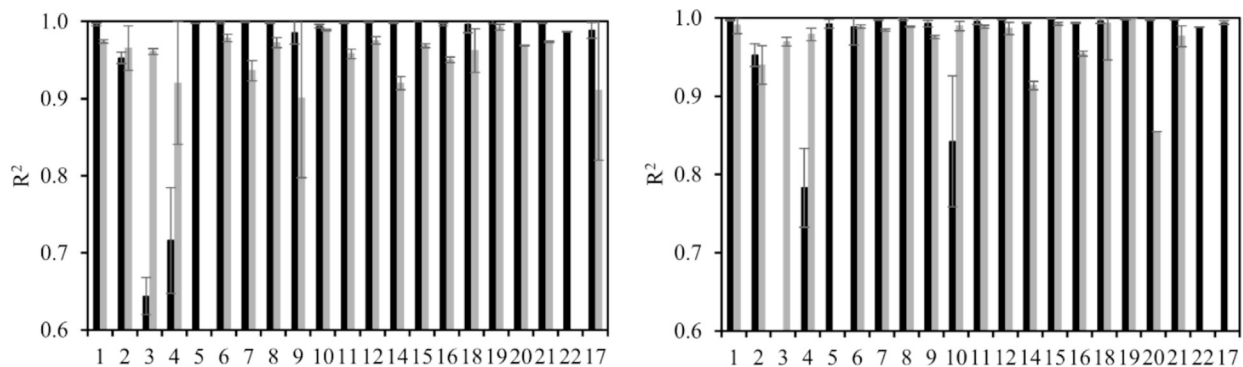


Fig. 7.  $R^2$  values for power law fits of dry (left) and wet (right) test data. Error bars indicate standard deviation.

Table 4

Average values and standard deviations of the averages of  $A$  and  $B$  across the 5 tests for each participant. Extrapolated thickness values at compaction stress values of 200 kPa and 300 kPa are also given. CV indicates coefficients of variation.

	dry loading	unloading	wet loading	unloading
$A / \text{mm}$	$3.13 \pm 0.48$	$3.00 \pm 0.11$	$3.23 \pm 0.23$	$3.03 \pm 0.10$
CV( $A$ )	15 %	4 %	7 %	3 %
$-100B$	$16.86 \pm 27.92$	$3.85 \pm 2.75$	$12.18 \pm 8.33$	$2.68 \pm 1.34$
CV( $B$ )	166 %	71 %	68 %	50 %
$t(200 \text{ kPa}) / \text{mm}$	$2.88 \pm 0.63$	$2.93 \pm 0.11$	$2.98 \pm 0.32$	$2.98 \pm 0.10$
CV( $t(200 \text{ kPa})$ )	22 %	4 %	11 %	3 %
$t(300 \text{ kPa}) / \text{mm}$	$2.76 \pm 0.68$	$2.88 \pm 0.12$	$2.85 \pm 0.36$	$2.95 \pm 0.10$
CV( $t(300 \text{ kPa})$ )	25 %	4 %	13 %	3 %

Table 5

Average values and standard deviations of the averages of  $A$  and  $B$  across the 5 tests for each participant, with the exception of the outliers, participants 3 and 4. Extrapolated thickness value at compaction stress values of 200 kPa and 300 kPa are also given. CV indicates coefficients of variation.

	dry loading	unloading	wet loading	unloading
$A / \text{mm}$	$3.27 \pm 0.15$	$3.00 \pm 0.11$	$3.28 \pm 0.17$	$3.03 \pm 0.10$
CV( $A$ )	4 %	4 %	5 %	3 %
$-100B$	$8.59 \pm 1.48$	$3.96 \pm 2.84$	$9.58 \pm 1.54$	$2.77 \pm 1.38$
CV( $B$ )	17 %	72 %	16 %	50 %
$t(200 \text{ kPa}) / \text{mm}$	$3.08 \pm 0.15$	$2.92 \pm 0.11$	$3.07 \pm 0.16$	$2.97 \pm 0.10$
CV( $t(200 \text{ kPa})$ )	5 %	4 %	5 %	3 %
$t(300 \text{ kPa}) / \text{mm}$	$2.97 \pm 0.16$	$2.87 \pm 0.12$	$2.95 \pm 0.17$	$2.94 \pm 0.10$
CV( $t(300 \text{ kPa})$ )	5 %	4 %	6 %	4 %

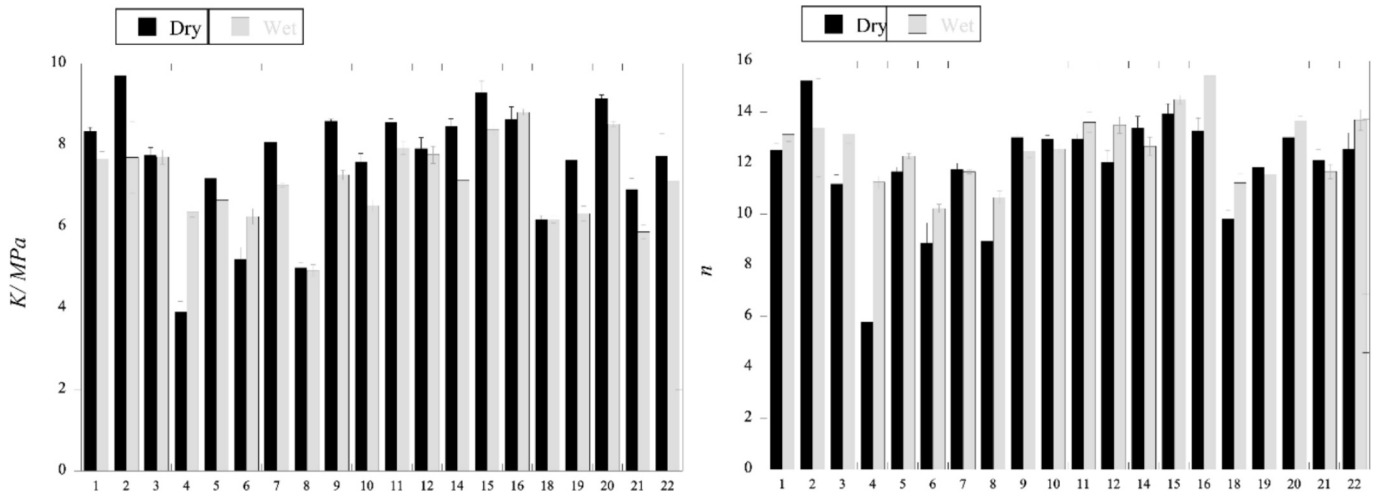


Fig. 8. Power law fit constants,  $K$  and  $n$ , for dry and wet test data. Error bars represent the standard deviation across the 5 tests for each participant.

a fabric behave as beams which can bend between contact points with other fibre bundles:

$$\sigma_c(V_f) = -C \frac{1 - \sqrt{\frac{V_f}{V_{f0}}}}{\left(\sqrt{\frac{V_a}{V_f}} - 1\right)^4}, C = \frac{3\pi E_f}{\beta^4} \quad (4)$$

In this model, the compaction stress is modelled as a function of the fibre volume fraction,  $V_f$ , which is in turn a function of the specimen thickness.  $V_{f0}$  and  $V_a$  are the initial uncompressed fibre volume fraction, and the maximum obtainable fibre volume fraction during compression, respectively. The constant  $C$  depends on the fibre bending stiffness, which is represented by the modulus,  $E_f$ , and a geometrical ratio for the fibre beam network ( $\beta = \text{span length} / \text{span height}$ ). In this study,  $C$  and  $V_a$  were obtained by fitting Eq. (4) to the data.

Again, any data for stress values under 1 kPa was excluded from the fits. At first,  $V_{f0}$  was set equal to the minimum fibre volume fraction in the remaining data (at  $\sim 1$  kPa in both loading and unloading) for each individual test sample. The fit qualities were seemingly low as a result, and this was thought to be related to the variation in values used for  $V_{f0}$ . Thus, a “standard” value was chosen for all tests and all participants, as the average minimum fibre volume fraction. The approximate averages used were 35 % and 40 % respectively for dry loading and unloading, and 35 % and 50 % for wet loading and unloading. Note the higher lubrication induced in the wet tests, as evident by higher fibre volume fraction values at the end of the loading–unloading cycle for each sample. The data was then re-screened, to only include data for fibre volume fractions above these values, with a hard limit excluding any

data below 1 Pa.

Fig. 9 shows the fitted values for the scalar constant  $C$ , for the dry test data. There was more variation in this fitted value than any of the other fitted constants in this study. There was also a significant difference in scale between this fitted constant for the loading and unloading data, thus Fig. 9 splits the chart into two charts with different scales.

Fig. 10 shows the fitted values for the maximum fibre volume fraction, as well as the  $R^2$  fit quality for each participant. The  $V_a$  fitted values above 100 % have no physical meaning, but seem to be outliers, where the average  $V_a$  is 91.5 % for loading and 65.9 % for unloading, including all outliers. The scatter in results seems to be much less than for the constant  $C$ .  $R^2$  values seem to be similarly good compared to the power law fit, especially for loading data, with lower fit quality in unloading.

The dry – wet differences in fit constants were once again minimal for loading data, with both the average  $C_{dry}/C_{wet}$  and  $V_{a,dry}/V_{a,wet}$  approximately equal to 0.95. For unloading, the differences in the scalar  $C$  were larger, with  $C_{dry}/C_{wet} = 0.44$  and  $V_{a,dry}/V_{a,wet} = 0.98$ .

### 5.2. Effect of specimen wetting

For compaction of wet specimens, the recorded stress does not only relate to the properties of the reinforcement. It also depends on the pressure required to squeeze the viscous fluid out of the porous reinforcement as the specimen thickness is reduced. The fluid pressure depends on the rate of compaction (1 mm/min), the reinforcement permeability (in the order of  $10^{-11}$  m<sup>2</sup>; decreases with increasing level of compaction, implying that the fluid pressure will increase during a compression test), the fluid viscosity (approximately 0.1 Pa.s), and also on the specimen size, which affects the length of fluid flow paths (radius

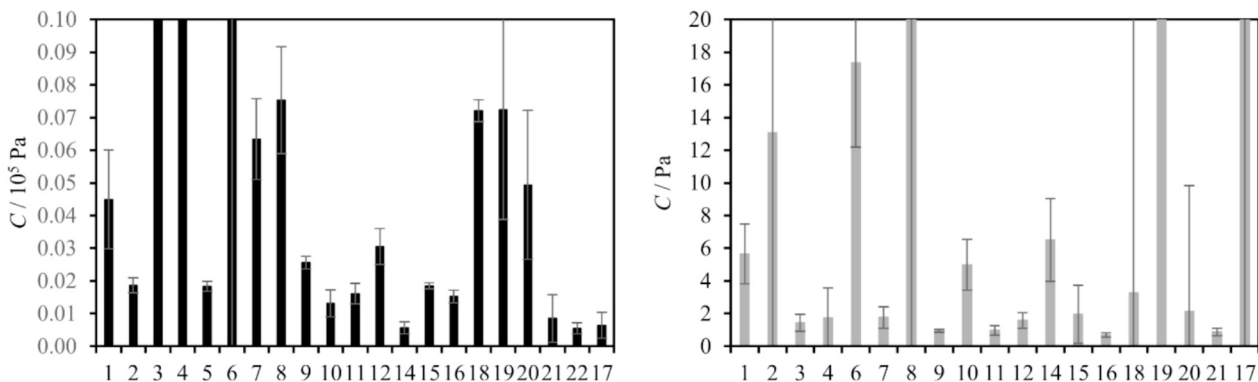


Fig. 9. Fitted constant  $C$  for the Gutowski model: dry loading data (left) and unloading data (right). Error bars represent standard deviation.

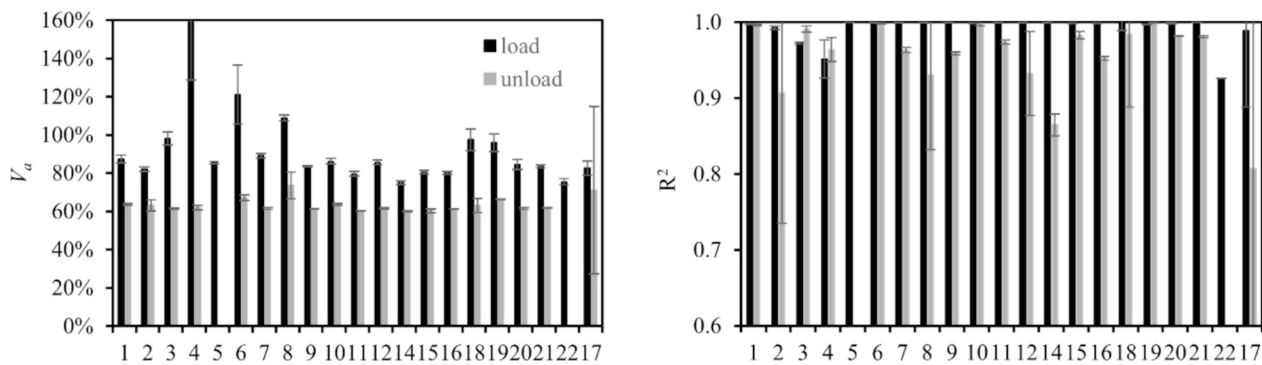


Fig. 10. Fitted values for  $V_a$  (left) and  $R^2$  (right), for Gutowski fits to dry data. Error bars represent standard deviation.

of circular specimens in the order of 0.05 m). Using equations derived elsewhere [31,32], a fluid pressure in the order of  $10^4$  Pa (averaged over the specimen size) is found at maximum specimen compression. Whilst this is not negligible, it is at least one order of magnitude smaller than typical stresses measured near maximum compression. However, the calculations assume that the specimens are fully wetted with no air inclusions. Whilst the level of wetting was not quantified prior to testing, this is not a plausible assumption for the tests discussed here, as the specimens were drained to remove excess fluid. Hence, the true effect of specimen wetting on the recorded compaction stress can be assumed to be much smaller for the data presented here. Nonetheless, this effect is to be kept in mind when defining compression speeds for testing.

### 5.3. Experimental issues

Parallelism of the compaction platens is essential for uniform compression of the reinforcement specimens. The majority of participants (17 out of 22) followed the guidelines and used set-ups with adjustable platens to ensure parallelism. In these set-ups, the bottom platen is typically rigidly connected to the base of the UTM. The top platen is connected to the load cell and cross-head through a spherical seat. Before a test is conducted, the platens are pressed together at a predefined load, such that the top platen can align with the bottom platen. Then, the spherically seated platen is fixated in position using locking screws. The load applied for aligning the platens was not prescribed here. For standardisation of the test method, a load corresponding to a pressure of  $10^5$  Pa will be proposed for consistency.

To map the distribution of the compaction stress between the platens (without a reinforcement specimen), 17 participants used pressure film (such as Fujifilm Prescale<sup>TM</sup>) which changes colour when a compaction stress is applied. Qualitatively, the results show that the stress distribution is never perfectly uniform. Most participants observed a stress maximum in the centre of the platen geometry, underneath the

connector to the UTM (Fig. 11.a). This could indicate that fixating the platens in position using locking screws may induce minor warping (if the locking screws are tightened too much). In general, the stress patterns suggest that non-uniformity is a result of platen flatness rather than misalignment.

If pressure film is applied between a compression platen and the reinforcement specimen, the observed stress distribution tends to be non-uniform on a small scale (Fig. 11.b) because of the textile pattern, which results in local variations in fibre volume fraction and compaction stiffness. On a global scale, the stress distribution tends to be more uniform (compared to platen-platen compression), as the reinforcement specimen levels out stress variations if the platens are not perfectly flat. This indicates that unavoidable minor issues with flatness of the platens are not a problem, as long as there are no systematic variations in compaction stress.

As highlighted elsewhere [18], the slope of the recorded  $\sigma_c(t)$  curves is steep at small values of  $t$ , i.e. at high compaction levels (see examples in Fig. 3). As a result, small uncertainties in the measured specimen thickness can have a large effect on the identified compaction stress. Hence, using a direct thickness measurement method is essential to minimise uncertainties in  $t$ . To avoid systematic offsets in  $t$ , the direct measurement of the thickness needs to be zeroed appropriately. Whilst this was not addressed in the guidelines for this study, it will be proposed in future standardisation to zero the displacement at the preload applied for aligning the compaction platens.

For three participants, offsets in  $\sigma_c$  occurred in the recorded  $\sigma_c(t)$  curves (i.e. non-zero values of the compaction stress when the specimens are not compacted). As discussed above, positive offsets in the compaction stress made fitting of compaction models to the recorded data difficult and resulted in data sets to be excluded from quantitative evaluation. In some cases, the compaction stress derived from the recorded force data showed negative values, which would correspond to tensile stresses in the specimen. As the specimens consist of separate

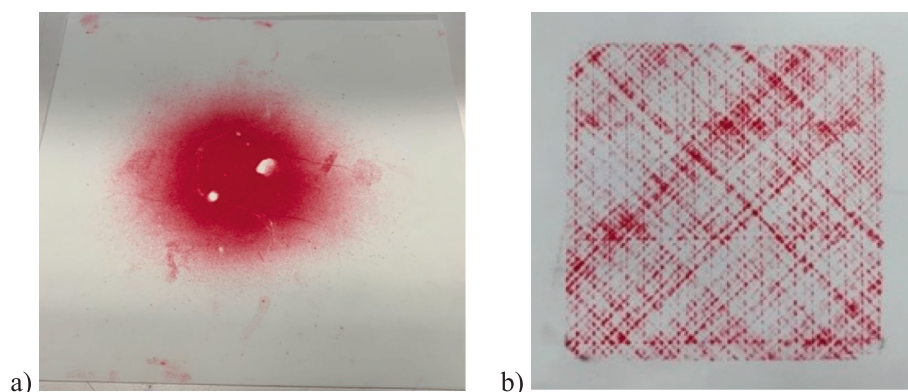


Fig. 11. Examples for recorded distributions of compaction stress. a) circular platen, no specimen; b) with reinforcement specimen.

fabric layers, this would be implausible behaviour. Recorded curves showing this behaviour were included in the evaluation, but they suggest that there may have been issues with zeroing the load cell.

In addition to purely experimental issues, the conversion from force values recorded at the UTM load cell to compaction stress values was incorrect in some data submitted by the participants. Similarly, the correct compaction stress is calculated by dividing the applied force by the specimen area, not the platen area (if the specimens are smaller than the platens). The values in question were corrected when all data were checked. This highlights again the effect of human error on the results [33], which can cause significantly higher scatter (values differ by a factor of 10 if the units, MPa and bar, are used inconsistently) than effects such as measurement inaccuracies (errors typically in the order of several percent).

One participant did not provide the requested information in their documentation of the compression tests (see Tables 2 and 3). As this means that experimental parameters are not traceable, the data set in question was counted as non-compliant with the guidelines.

#### 5.4. ANOVA analysis of the variables

In order to assess the impact of different variables within the test setup, an ANOVA analysis was carried out. This statistical test allows the comparison of multiple variables and assesses their impact. The p-values for the hypothesis “the data are not affected by the factor” are shown in Table 6. This statistical method was used to assess the impact of the following:

- Type of thickness sensor: use of LVDT or alternative method
- Compliance with all of the following guidelines:
  - o Fabric cut with CNC or die cutter
  - o Use of UTM for testing
  - o Use of self-aligning platen
  - o Use of pressure film prior to testing
  - o Use of a direct thickness sensor
  - o Use of a smaller platen than specimen

It was not possible to carry out the ANOVA analysis on the effect of each guideline and type of thickness sensor individually due to the disproportionate number of “yes” values for compliance to each variable, which caused the “yes” and “no” groups to be unbalanced. This feature can make the outcome of the analysis more sensitive to the “no” values, i.e. the smaller group. To compensate for the unbalanced groups, the variables were further grouped into the bundles compliant/not compliant with the guidelines and use of LVDT/not-LVDT for thickness measurement. These variables were assessed for their impact on the thickness at  $10^5$  Pa compaction stress and the constant,  $B$ , from the power law fit data.

Tests carried out using the “anovan” function in MATLAB on the full data sets showed that neither of the bundled factors affected the results. The p-values (i.e. the probability that the given statistic result would be generated if the factors have no effect on the measured value) are given for each factor and measurement in Table 6. Here, we would only reject the hypothesis if the p-values are low, e.g. 0.01. As the p-values here are large, we can conclude that effects of the respective factors on the data

**Table 6**  
Results of ANOVA analysis (p-values) for different test variables.

	Compliance to guidelines	Thickness measurement (LVDT)
$B$ , compression, wet	0.05	0.48
$B$ , relaxation, wet	0.16	0.89
$B$ , compression, dry	0.07	0.59
$B$ , relaxation, dry	0.46	0.28
$A$ , dry	0.96	0.60
$A$ , wet	0.27	0.96

are unlikely. It should be noted that due to participants 3 and 4 being outliers in the data for “ $B$ , comp”, the results for these values may be unreliable. While the ANOVA analysis was unable to show any significant impact from these variables, the importance of providing a best-practice method in order to minimise the methodological errors, as well as ensuring measurement precision, remains [34].

#### 5.5. Compliance with guidelines

The effect of compliance/non-compliance of participants’ test procedures with the guidelines on the consistency of results was assessed based on two descriptors:

- Focusing on the specimen thickness at a compaction stress of  $10^5$  Pa, two participants, 13 and 17, are ignored (see above). For participant 18, compliance could not be verified, hence the procedure was counted as non-compliant. This leaves 13 participants with compliant procedures, and 6 participants with non-compliant procedures. For the group of participants who complied with the guidelines, the CV of  $t(10^5$  Pa) is 4 % and 5 % for dry and wet tests, respectively. For participants employing non-compliant procedures, the CV is 3 % for dry tests and 2 % for wet tests. This means that, based on this single-point comparison, the scatter in values of the thickness at an applied compaction stress of  $10^5$  Pa is in the same order for compliant and non-compliant procedures.
- Evaluating the power-law fits to the recorded data, the average values and standard deviations of the averages of  $A$  and  $B$  across the 5 tests are given in Tables 7 and 8 for participants using compliant and non-compliant procedures. In addition, the corresponding coefficients of variation are given. Participant 13 was again not considered as the recorded curves were not provided, and participant 18 was again counted as non-compliant. The two outliers, participants 3 and 4 (both non-compliant) were not considered as the power-law fits showed poor quality because of offsets in  $\sigma_c$ . The results (13 compliant and 6 non-compliant) listed in the tables show that, as the factor  $A$  is equivalent to  $t(10^5$  Pa), the CV of  $A$  is very similar to that of the measured  $t(10^5$  Pa). For curves recorded in loading (dry and wet), the CV of  $A$  is approximately the same for compliant as for non-compliant procedures. The CV of  $B$  is lower for compliant than for non-compliant procedures. In unloading (dry and wet), non-compliant procedures result in lower CV of  $A$  and  $B$  than compliant procedures.

In summary, there is no clear reduction of scatter in results for compliant test procedures compared to non-compliant procedures. However, with the exception of participant 17, the non-compliant procedures typically only deviate from the guidelines in one or two aspects (see Table 3). This appears generally not enough to cause a significant difference in average results and their variability.

Comparison of the variability in results with that from a previous study, where the guidelines were less prescriptive [6], shows that the CV of the maximum compaction stress for the dry and wet tests is of the same order. Here, it is 46 % and 42 %, respectively. In the previous study, it was between 38 % to 50 % for two different fabrics. The CV of

**Table 7**  
Average values and standard deviations of the averages of  $A$  and  $B$  across the 5 tests for participants who complied with the guidelines. CV indicates coefficients of variation.

	dry loading	unloading	wet loading	unloading
$A$ / mm	$3.27 \pm 0.14$	$2.99 \pm 0.14$	$3.29 \pm 0.17$	$3.03 \pm 0.12$
CV( $A$ )	4 %	5 %	5 %	4 %
-100 $B$	$8.54 \pm 1.32$	$3.94 \pm 3.17$	$9.31 \pm 1.05$	$2.87 \pm 1.49$
CV( $B$ )	15 %	80 %	11 %	52 %

**Table 8**

Average values and standard deviations of the averages of *A* and *B* across the 5 tests for participants who did not comply with the guidelines. CV indicates coefficients of variation.

	dry		wet	
	loading	unloading	loading	unloading
<i>A</i> / mm	3.25 ± 0.17	3.01 ± 0.04	3.24 ± 0.16	3.03 ± 0.03
CV( <i>A</i> )	5 %	1 %	5 %	1 %
-100 <i>B</i>	8.68 ± 1.92	4.01 ± 2.24	10.17 ± 2.30	2.55 ± 1.21
CV( <i>B</i> )	22 %	56 %	23 %	47 %

the specimen thickness at a compaction stress of  $10^5$  Pa was also in a similar range (between 2 % and 4 %) as here.

While the guidelines should help to improve the accuracy of controlling and measuring the test parameters for the compaction tests, possible reasons for the lack of a significant reduction in scatter are:

- Misinterpretation of the guidelines or inappropriate implementation of apparently compliant procedures (human error).
- Variability in specimen properties (related to material storage, specimen cutting and handling, which may result in pre-compaction of the fabric) having a strong effect on the compaction response.

## 6. Conclusions

In this benchmark exercise, 22 participants submitted measured data for the thickness and compaction stress changes of glass fibre fabric specimens compressed to a thickness of 3 mm following a prescribed test profile. One of the participants compressed the specimens using a vacuum bag, while the remaining 21 carried out the tests using a universal test machine. Detailed guidelines for the test setup were provided in order to assess whether the proposed test method was suitable, i.e. practical and precise, for publication as a test standard. Despite the mandatory target specimen thickness of 3 mm, results showed enough deviation from the target thickness at maximum compaction to make comparison of the maximum stress difficult.

Hence, values of measured thickness at  $10^5$  Pa pressure were compared, and here the CV between participants was found to be 4 % for both wet and dry tests.

To overcome the limitations of comparing results based on a single point on the compaction curves, a power law model and a model proposed by Gutowski were fitted to the recorded data. Both models produced generally fits of a good quality, i.e. high values of  $R^2$ . As the power law model is easier to fit, it was used for description of recorded data in terms of the two parameters appearing in the model. Based on these parameters, compaction curves obtained in procedures complying with all guidelines did not show a clearly reduced variability compared to procedures not complying with all guidelines.

While the data showed good reproducibility when normalised to the same pressure value, the steepness of the curves at higher levels of compression present a risk that small changes in thickness result in large differences in reported pressure values. Consequently, it will be recommended in the procedure for standardisation that data be fitted using the power law model, which has been shown here to be a reliable and reproducible approach.

As the guidelines are expected to minimise inaccuracies in the test method, it can be speculated that the residual scatter in results is caused by issues with the implementation of the procedures, undefined approaches to UTM calibration, and by variability in the specimen properties. While these are potential topics for future work, the following guidelines will be proposed as a test protocol for standardisation:

- The specimens shall have an edge length (if square or rectangular) or diameter (if round) in the order of 100 mm. The compaction platens shall be larger than the test specimens.
- Fabric layers shall be assembled into a stack prior to cutting and cut to size using a precise method such as a die cutter or CNC. Specimens shall be stacked carefully to minimise fraying and incorrect alignment.
- Tests shall be carried out using a calibrated Universal Test Machine. The test machine shall be fitted with a lockable self-aligning platen, with compression platens of larger surface area than the specimen. The distance between the platens shall be measured using a direct method.
- Prior to testing, the platens shall be pressed together at a defined load before they are fixated. The displacement shall be zeroed at this load. A parallelism check shall be carried out using pressure film. The force readings shall be zero when the specimens are not compacted.
- The same loading and unloading speed shall be used for each test in a series.
- For wet tests, all specimens in a test series shall be soaked and drained for the same amount of time prior to testing.
- All test details shall be recorded and reported.

## CRedit authorship contribution statement

**A.X.H. Yong:** Writing – original draft, Project administration, Methodology, Formal analysis, Data curation, Conceptualization. **A. Endruweit:** Writing – original draft, Methodology, Investigation, Formal analysis. **A. George:** Writing – original draft, Investigation, Formal analysis. **D. May:** Writing – original draft, Methodology, Investigation, Formal analysis. **Y.A. Aksoy:** Investigation. **M.A. Ali:** Investigation. **T. Allen:** Investigation. **M. Bender:** Investigation. **M. Bodaghi:** Investigation. **B. Caglar:** Investigation. **H. Caglar:** Investigation. **A. Chiminelli:** Investigation. **S. Comas-Cardona:** Investigation. **R. de Ribains:** Investigation. **J. Dittmann:** Investigation. **C. Dransfeld:** Investigation. **E. Fauster:** Investigation. **A. Guilloux:** Investigation. **P. Hubert:** Methodology, Investigation. **S. Idapalapati:** Investigation. **J. Ivens:** Investigation. **J. Janzen:** Investigation. **Y. Jiang:** Investigation. **T. Khan:** Investigation. **M. Laspalas:** Investigation. **F. LeBel:** Investigation. **J. Lee:** Investigation. **X. Liu:** Investigation. **M. Lizaranzu:** Investigation. **S.V. Lomov:** Methodology, Investigation. **C. López:** Investigation. **K. Masania:** Investigation. **V. Michaud:** Writing – original draft, Investigation, Formal analysis. **P. Middendorf:** Investigation. **S. Miguel:** Investigation. **S.S. Narayana:** Investigation. **C.H. Park:** Investigation. **S. Ravisankar Padma:** Investigation. **L. Riffard:** Investigation. **C. Pinger:** Investigation. **V. Rougier:** Investigation. **H. Sas:** Investigation. **D. Sayinbas:** Investigation. **P. Sousa:** Investigation. **M. Sozer:** Investigation. **M. Steinhardt:** Investigation. **R. Umer:** Investigation. **J.D. Vincent:** Investigation. **V. Werlen:** Investigation. **O. Yuksel:** Investigation.

## Declaration of competing interest

The authors declare that they have no known competing financial interests or personal relationships that could have appeared to influence the work reported in this paper.

## Acknowledgements

ITA participation in this benchmark has been possible thanks to the support of the European Regional Development Fund (ERDF) for Aragon region (Spain).

## Appendix A

Table A1

Platen and sample dimensions.

ID	Platen Shape	Length	Width	Diameter	Sample Shape	Length	Width	Diameter
1	Circle	--	--	100	Circle	--	--	90
2	Circle	--	--	250	Square	150	150	--
3	Square	152.4	63.5	--	Square	55	55	--
4	Other	80	55	--	Other	80	50	--
5	Circle	--	--	200	Square	100	100	--
6	Circle	--	--	130	Circle	--	--	100
7	Circle	--	--	150	Circle	--	--	130
8	Circle	--	--	135	Circle	--	--	100
9	Square	220	220	--	Square	100	100	--
10	Square	200	200	--	Square	100	100	--
11	Circle	--	--	177	Circle	--	--	100
12		--	--	--	Square	100	100	--
13	Circle	--	--	156	Square	100	100	--
14	Circle	--	--	136	Circle	--	--	100
15	Circle	--	--	135	Square	90	90	--
16	Circle	--	--	135	Circle	--	--	100
17	N/A	N/A	N/A	N/A	Circle	--	--	98
18	Circle	--	--	150	Circle	--	--	90
19	Circle	--	--	150	Circle	--	--	100
20	Circle	--	--	150	Circle	--	--	132
21	Circle	--	--	140	Circle	--	--	80
22	Square	107	107	--	Circle	--	--	100

## Data availability

Data will be made available on request.

## References

- [1] Robitaille F, Gauvin R. Compaction of textile reinforcements for composites manufacturing. I: Review of experimental results. *Polym Compos* 1998;19(2): 198–216.
- [2] Batch GL, Cumiskey S, Macosko CW. Compaction of fiber reinforcements. *Polym Compos* 2002;23(3):307–18.
- [3] Bickerton S, Buntain MJ, Somashekar AA. The viscoelastic compression behavior of liquid composite molding preforms. *Compos A Appl Sci Manuf* 2003;34(5):431–44.
- [4] Werlen, A numerical approach to characterize the viscoelastic behaviour of fibre beds and to evaluate the influence of strain deviations on viscoelastic parameter extraction *Composites: Part A: Applied Science and Manufacturing*, 2021; **143**: 106315.
- [5] Kelly PA. A viscoelastic model for the compaction of fibrous materials. *J Text Inst* 2011;102(8):689–99.
- [6] Somashekar AA, Bickerton S, Bhattacharyya D. Modelling the viscoelastic stress relaxation of glass fibre reinforcements under constant compaction strain during composites manufacturing. *Composites A: Applied Science and Manufacturing* 2012;43(7):1044–52.
- [7] Vangheluwe L, Kiekens P. Modelling relaxation behaviour of yarns part I: Extended, nonlinear maxwell model. *J Text Inst* 1996;87(2):296–304.
- [8] Kabachi M, Danzi M, Arreguin S, Ermanni P. Experimental study on the influence of cyclic compaction on the fiber-bed permeability, quasi-static and dynamic compaction responses. *Composites A: Applied Science and Manufacturing*; 2019. p. 125.
- [9] Servais C, Michaud V, Månson J-A-E. The packing stress of impregnated fiber mats. *Polym Compos* 2001;22(2):298–311.
- [10] Danzi M, Schneberger C, Ermanni P. A model for the time-dependent compaction response of woven fiber textiles. *Composites A: Applied Science and Manufacturing* 2018;105:180–8.
- [11] Toll S. Packing mechanics of fiber reinforcements. *Polym Eng Sci* 1998;38(8): 1337–50.
- [12] Kim YR, McCarthy SP, Fanucci JP. Compressibility and relaxation of fiber reinforcements during composite processing. *Polym Compos* 1991;12(1):13–9.
- [13] Wei K, Liang D, Mei M, Yang X, Chen L. A viscoelastic model of compression and relaxation behaviors in preforming process for carbon fiber fabrics with binder. *Compos B Eng* 2019;158:1–9.
- [14] Saunders R, Lekakou C, Bader M. Compression in the processing of polymer composites 2. Modelling of the viscoelastic compression of resin-impregnated fibre networks. *Compos Sci Technol* 1999;59:1483–94.
- [15] Pillai KM, Phelan FR, Tucker CL. Numerical simulation of Injection/Compression Liquid Composite Molding. Part 2: Preform Compression. *Compos A Appl Sci Manuf* 2001;32(2):207–20.
- [16] Trevino L, Rupel K, Young WB, Liou MJ, Lee LJ. Analysis of resin injection molding in molds with preplaced fiber mats. I: Permeability and compressibility measurements. *Polym Compos* 1991;12(1):20–9.
- [17] Chen B, Chou TW. Compaction of woven-fabric preforms: nesting and multi-layer deformation. *Compos Sci Technol* 2000;60(12–13):2223–31.
- [18] Yong AXH, Aktas A, May D, Endruweit A, Lomov SV, Advani S, et al. Experimental characterisation of textile compaction response: a benchmark exercise. *Compos A Appl Sci Manuf* 2021;142:106243.
- [19] May D, Aktas A, Advani SG, Berg DC, Endruweit A, Fauster E, et al. In-plane permeability characterization of engineering textiles based on radial flow experiments: a benchmark exercise. *Compos A Appl Sci Manuf* 2019;121:100–14.
- [20] Yong AXH, Endruweit A, George A, May D, Aksoy YA, Ali MA, et al. Towards standardisation of the out-of-plane permeability measurement for reinforcement textiles. *Compos A Appl Sci Manuf* 2025;190:108630.
- [21] Yong AXH, Aktas A, May D, Endruweit A, Advani S, Hubert P, et al. Out-of-plane permeability measurement for reinforcement textiles: a benchmark exercise. *Compos A Appl Sci Manuf* 2021;148:106480.
- [22] Pearce N, Summerscales J. The compressibility of a reinforcement fabric. *Compos Manuf* 1995;6(1):15–21.
- [23] Sousa P, Lomov SV, Ivens J. Methodology of dry and wet compressibility measurement. *Compos A Appl Sci Manuf* 2020;128:105672.
- [24] Sousa P, Liu X, Lomov SV, Ivens J. Achieving highly accurate cavity thickness measurements in fabric compaction. *J Compos Mater* 2024;58(8):1089–105.
- [25] Kelly PA, Umer R, Bickerton S. Viscoelastic response of dry and wet fibrous materials during infusion processes. *Compos A Appl Sci Manuf* 2006;37(6):868–73.
- [26] Gutowski TG, Cai Z, Bauer S, Boucher D, Kingery J, Wineman S. Consolidation experiments for laminate composites. *J Compos Mater* 1987;21(7):650–69.
- [27] Wyk CM. Note on the Compressibility of Wool. *Journal of the Textile Institute Transactions* 1946;37(12):T285–92.
- [28] Toll S, Månson J-A. *Elastic Compression of a Fiber Network*. *J Appl Mech* 1995;62.
- [29] Alkhagen M, Toll S. Micromechanics of a compressed fiber mass. *J Appl Mech* 2007;74:723–73.
- [30] Latil P, Orgéas L, Geindreau C, Dumont PJJ, Rolland du Roscoat S. Towards the 3D in situ characterisation of deformation micro-mechanisms within a compressed bundle of fibres. *Compos Sci Technol* 2011;71(4):480–8.
- [31] Buntain MJ, Bickerton S. Compression flow permeability measurement: a continuous technique. *Compos A Appl Sci Manuf* 2003;34(5):445–57.

- [32] Comas-Cardona S, Binetruy C, Krawczak P. Unidirectional compression of fibre reinforcements. Part 2: a continuous permeability tensor measurement. *Composites Science and Technology* 2007;67(3–4):638–45.
- [33] Arbter R, Beraud JM, Binetruy C, Bizet L, Bréard J, Comas-Cardona S, et al. Experimental determination of the permeability of textiles: a benchmark exercise. *Compos A Appl Sci Manuf* 2011;42(9):1157–68.
- [34] May D, Advani SG, Duhovic M, Endruweit A, Fauster E, George A, et al. A new ISO standard for the experimental characterization of in-plane permeability of fibrous reinforcements. *Compos A Appl Sci Manuf* 2025;190:108592.